

# Coupling hydrophobic, dispersion, and electrostatic contributions in continuum solvent models

J. Dzubiella,\* J. M. J. Swanson, and J. A. McCammon

*NSF Center for Theoretical Biological Physics (CTBP), and*

*Department of Chemistry and Biochemistry,*

*University of California, San Diego, La Jolla, California 92093-0365*

(Dated: August 3, 2018)

## Abstract

Recent studies of the hydration of micro- and nanoscale solutes have demonstrated a strong *coupling* between hydrophobic, dispersion and electrostatic contributions, a fact not accounted for in current implicit solvent models. We present a theoretical formalism which accounts for coupling by minimizing the Gibbs free energy with respect to a solvent volume exclusion function. The solvent accessible surface is output of our theory. Our method is illustrated with the hydration of alkane-assembled solutes on different length scales, and captures the strong sensitivity to the particular form of the solute-solvent interactions in agreement with recent computer simulations.

---

\*e-mail address: jdzubiella@ucsd.edu

Much progress has been made in the last decade in the understanding of hydrophobic solvation on different length scales [1, 2]. Most of this work has been devoted to study solvation of purely repulsive, hard sphere-like solutes, while less attention has been given to the influence and incorporation of dispersion or electrostatic contributions. Likewise, an entire field in the biophysical community has explored electrostatic solvation effects in the absence or uncoupled addition to hydrophobic considerations [3]. Recently, however, several computer simulations have demonstrated a strong coupling between hydrophobicity, solute-solvent dispersion attractions, and electrostatics. For example, a simulation of explicit water between paraffin plates revealed that hydrophobic attraction and dewetting phenomena are strongly sensitive to the nature of solute-solvent dispersion interactions [4]. Similarly, simulations of hydrophobic channels [5, 6] and nanosolutes [7] have shown that charged solutes, which attract the dipolar solvent due to increasing electric field strength close to the solute surface, strongly affect the dewetting behavior and potentials of mean force (pmf). A fully atomistic simulation of the folding of the two-domain protein BphC enzyme [8] further supported coupling by showing that the region between the two domains was completely dewetted when solvent-solute van der Waals (vdW) and electrostatic interactions were turned off, but accommodated 30% of the density of bulk water with the addition of vdW attractions, and 85-90% with the addition of electrostatics, in accord with experimental results. Finally, Liu *et al.* recently observed a dewetting transition in the collapse of the melittin tetramer which was strongly sensitive to the type and location of the hydrophobic residues proving that these observations apply to realistic biomolecular systems [9].

In this letter we propose a continuum description of solvation that explicitly couples hydrophobic, dispersion and electrostatic contributions. Similar to the approach of Parker *et al.* in their study of bubble formation at hydrophobic surfaces [10], we express the Gibbs free energy as a functional of the solute cavity shape, the latter given by the volume exclusion function of the solvent, and obtain the optimal shape by minimization. This leads to an expression similar to the Laplace-Young equation for the geometrical description of capillary surfaces [11], but in contrast to existing approaches *explicitly* includes the inhomogeneous distributions of dispersion and electrostatic contributions as well as curvature corrections. Geometry-based approaches similar to our formalism exist in related fields, such as the Helfrich description of membranes shapes [11], wetting in colloids and granular media [11], and electrowetting [12]. We stress that, as opposed to other implicit solvent models [3],

the solvent accessible surface (SAS) is an output of our theory. This surface encloses the optimal solvent accessible volume and should not be confused with the canonical SAS [3] which is simply the union of probe-inflated spheres. We begin by verifying that our method is able to describe the solvation of small alkanes on molecular scales. We then demonstrate that it captures the strong sensitivity of dewetting and hydrophobic hydration to solute-solvent interactions on larger scales for a model system of two alkane-assembled spheres. In this striking example the strong hydrophobic attraction decreases almost two orders of magnitude in units of the thermal energy,  $k_B T$ , and dewetting is partially or completely suppressed when realistic dispersion and electrostatic contributions are included. We expect our approach to be particularly useful in solvation studies of proteins where the hydrophobic surfaces are highly irregular and laced with hydrophilic units, and a unified description of hydration on different length scales is important [1, 9, 13].

Let us consider an assembly of solutes with arbitrary shape and composition surrounded by a dielectric solvent in a macroscopic volume  $\mathcal{W}$ . We define a subvolume  $\mathcal{V}$  empty of solvent for which we can assign a volume exclusion function in space given by  $v(\vec{r}) = 0$  for  $r \in \mathcal{V}$  and  $v(\vec{r}) = 1$  elsewhere. We assume that the surface bounding the volume is continuous and closed. The absolute volume  $V$  and surface  $S$  of  $\mathcal{V}$  can then be expressed as functionals of  $v(\vec{r})$  via  $V[v] = \int_{\mathcal{W}} d^3r [1 - v(\vec{r})]$  and  $S[v] = \int_{\mathcal{W}} d^3r |\nabla v(\vec{r})|$ , where  $\nabla \equiv \nabla_{\vec{r}}$  is the usual gradient operator. The density distribution of the solvent is given by  $\rho(v(\vec{r})) = \rho_0 v(\vec{r})$ , where  $\rho_0$  is the bulk density of the solvent at fixed temperature and pressure. The solutes' positions and conformations are fixed.

We suggest expressing the Gibbs free energy  $G[v]$  of the system as a *functional* of  $v(\vec{r})$  and obtaining the optimal volume and surface via minimization  $\delta G[v]/\delta v[\vec{r}] = 0$ . We adopt the following ansatz for the Gibbs free energy:

$$G[v] = PV[v] + \int_{\mathcal{W}} d^3r \gamma(v) |\nabla v(\vec{r})| + \int_{\mathcal{W}} d^3r \rho(v) U(\vec{r}) + \frac{\epsilon_0}{2} \int_{\mathcal{W}} d^3r \{\nabla \Psi(v)\}^2 \epsilon(v). \quad (1)$$

The first term in (1) is the energy of creating a cavity in the solvent against the difference in bulk pressure between the liquid and vapor,  $P = P_l - P_v$ . The second term describes the energetic cost due to solvent rearrangement close to the cavity surface in terms of a coefficient  $\gamma$ . This interfacial energy penalty is thought to be the main driving force for hydrophobic phenomena [1]. The coefficient  $\gamma$  is not only a solvent specific quantity but also

depends on the local topology of the surface [13], i.e., it is a function of the volume exclusion function,  $\gamma = \gamma(v(\vec{r}))$ . The exact form of this function is not known. For planar macroscopic solvent-cavity interfaces  $\gamma$  is usually identified by the liquid-vapor surface tension,  $\gamma_{lv}$ , of the solvent, which we will also employ here. In the following we make a *local curvature approximation*, i.e. we assume that  $\gamma$  can be expressed solely as a function of the local mean curvature of the interface defined by  $v$ ,  $\gamma(v(\vec{r})) = \gamma(H(\vec{r}))$ , with  $H(\vec{r}) = (\kappa_1(\vec{r}) + \kappa_2(\vec{r}))/2$ , where  $\kappa_1$  and  $\kappa_2$  are the two principal curvatures. We then apply the first order curvature correction to  $\gamma$  given by scaled-particle theory [14], the commonly used ansatz to study the solvation of hard spheres, arriving at

$$\gamma(H(\vec{r})) = \gamma_{lv}(1 + 2\delta H(\vec{r})), \quad (2)$$

where  $\delta$  is a constant and positive length expected to be of the order of the solvent particle size [14]. The curvature is positive or negative for concave or convex surfaces, respectively. Note that this leads to an increased surface tension for concave surfaces, in agreement with the arguments of Nicholls *et al.* [15] in their study of alkanes. It has been shown by simulations that (2) predicts the interfacial energy of growing a spherical cavity in water rather well for radii  $\gtrsim 3\text{\AA}$  [16].

The third term in (1) is the total energy of the non-electrostatic solute-solvent interaction given a density distribution  $\rho(v)$ . The energy  $U(\vec{r}) = \sum_i U_i(\vec{r})$  is the sum of the short-ranged repulsive and long-ranged (attractive) dispersion interactions  $U_i$  between each solute atom  $i$  and a solvent molecule. Classical solvation studies typically represent  $U_i$  as an isotropic Lennard-Jones (LJ) potential,  $U_{LJ}(r) = 4\epsilon[(\sigma/r)^{12} - (\sigma/r)^6]$ , with an energy scale  $\epsilon$  and a length scale  $\sigma$ . The importance of treating dispersion interactions independently as opposed to absorbing them in to the surface tension term, has been emphasized by Gallicchio *et al.* in their study of cyclic alkanes [17].

The fourth term in (1) describes the total energy of the electrostatic field expressed by the local electrostatic potential  $\Psi(v(\vec{r}))$  and the position-dependent dielectric constant  $\epsilon(\vec{r})$  assuming linear response of the dielectric solvent. In general, the electrostatic potential  $\Psi$  can be evaluated by Poisson's equation,  $\nabla \cdot [\epsilon(\vec{r})\nabla\Psi(\vec{r})] = -\lambda(\vec{r})/\epsilon_0$ , where  $\lambda(\vec{r})$  is the solute's charge density distribution. The most common form for the dielectric function,  $\epsilon(\vec{r})$ , is proportional to the volume exclusion function  $v(\vec{r})$  [3]

$$\epsilon(v(\vec{r})) = \epsilon_v + v(\vec{r})(\epsilon_l - \epsilon_v), \quad (3)$$

where  $\epsilon_v$  and  $\epsilon_l$  are the dielectric constants inside and outside the volume  $\mathcal{V}$ , respectively.

Plugging in (2) and (3) in functional (1) and using the calculus of functional derivatives, the minimization yields

$$0 = P - 2\gamma_{lv} [H(\vec{r}) + \delta K(\vec{r})] - \rho_0 U(\vec{r}) - \frac{\epsilon_0}{2} [\nabla \Psi(\vec{r}) \epsilon(\vec{r})]^2 \left( \frac{1}{\epsilon_l} - \frac{1}{\epsilon_v} \right). \quad (4)$$

Eq. (4) is an ordinary second order differential equation for the optimal solvent accessible volume and surface expressed in terms of pressure, surface curvatures, dispersion interactions, and electrostatics, all of which have dimensions of force per surface area or energy density.  $K(\vec{r}) = \kappa_1(\vec{r})\kappa_2(\vec{r})$  is the Gaussian curvature and follows from the variation of the surface integral over  $H(\vec{r})$  in (1). Thus, in our approach the geometry of the surface, expressed by  $H$  and  $K$ , is directly related to the inhomogeneous dispersion and electrostatic energy contributions. Note that the SAS is presently defined with respect to the LJ centers of the solvent molecules.

In the following we illustrate solutions of (4) in spherical and cylindrical symmetries. For a spherical solute (4) reduces to a function of  $R$ , the radius of the solvent accessible sphere,  $H = -1/R$  and  $K = 1/R^2$ . In cylindrical symmetry the SAS can be expressed by a one dimensional shape function  $r(z)$ , where  $z$  is the coordinate on the symmetry axis in  $z$ -direction and  $r$  the radial distance to it. The three-dimensional surface is obtained by revolving  $r(z)$  around the symmetry axis. We express  $r = r(t)$  and  $z = z(t)$  as functions of the parameter  $t$ . The principal curvatures are then given by  $\kappa_1 = -z'/(r\sqrt{r'^2 + z'^2})$  and  $\kappa_2 = (z'r'' - z''r')/((r'^2 + z'^2)^{3/2})$ , where the primes indicate the partial derivative with respect to  $t$ . We solve (4) and Poisson's equation numerically, using standard forward time relaxation schemes.

We now study the solvation of methane and ethane in water and compare our results to the SPC explicit water simulations by Ashbaugh *et al.* [18], in which the alkanes are modeled by neutral LJ spheres. The LJ water-atom parameters are  $\epsilon = 0.8941\text{kJ/mol}$  and  $\sigma = 3.45\text{\AA}$  for  $\text{CH}_4$ , and  $\epsilon = 0.7503\text{kJ/mol}$  and  $\sigma = 3.47\text{\AA}$  for  $\text{CH}_3$ , and the bond length of ethane is  $1.53\text{\AA}$ . We fix the liquid-vapor surface tension for SPC water at 300K to  $\gamma_{lv} = 65\text{mJ/m}^2$  [16]. Since we deal with water under ambient conditions the pressure term can be neglected and the length  $\delta$  remains the only free parameter. For methane we can reproduce the simulation solvation energy with a fit  $\delta = 0.85\text{\AA}$ . This is in good agreement with Huang *et al.* [16] who measured  $\delta = 0.76 \pm 0.05\text{\AA}$  for SPC water. Solving

the cylindrically symmetric problem for the diatomic ethane with the same  $\delta = 0.85\text{\AA}$ , we obtain a fit-parameter-free  $G = 11.48\text{kJ/mol}$ , which is only 7% larger than the simulation results. Alternatively, the best fit  $\delta = 0.87\text{\AA}$  reproduces the simulation energy exactly. This is surprisingly good agreement given the crude curvature correction we apply and the fact that the large curvature of the system varies locally in space. This supports the validity of our continuum approach down to a molecular scale. The curvature and shape functions  $H(z)$ ,  $K(z)$ , and  $r(z)$  are plotted in Fig. 1 together with the vdW surface and the canonical SAS obtained from rolling a probe sphere with a typically chosen radius  $r_p = 1.4\text{\AA}$  over the vdW surface [3]. Away from the center of mass  $|z| \gtrsim 1\text{\AA}$  the curvatures follow the expected trends  $H \simeq -1/R$  and  $K \simeq 1/R^2$  with  $R \simeq 3.1\text{\AA}$  for the spherical surfaces. The surface resulting from our theory is smaller than the canonical SAS, and is smooth at the center of mass ( $z = 0$ ) where the canonical SAS has a kink. Thus our surface has a smaller mean curvature at  $z = 0$  and an almost zero Gaussian curvature, which is typical for a cylinder geometry for which one of the principal curvatures is zero. These results may justify the use of smooth surfaces in coarse-grained models of closely-packed hydrocarbon surfaces, a possibility we will now explore with solvation on larger length scales where dewetting effects can occur.

Let us consider two spherical solutes which we assume to be homogeneously assembled of  $\text{CH}_2$  groups with a uniform density  $\rho = 0.024\text{\AA}^{-3}$  up to a radius  $R_0 = 15\text{\AA}$ , defined by the maximal distance between a  $\text{CH}_2$  center and the center of the solute. The  $\text{CH}_2$ -water LJ parameters are  $\epsilon = 0.5665\text{kJ/mol}$  and  $\sigma = 3.536\text{\AA}$ . Similar ones have been used by Huang *et al.* [4] to study dewetting between paraffin plates. The integration of the  $\text{CH}_2$ -water LJ interaction over the volume of a sphere leads yields a 9-3 like potential for the interaction between the center of the paraffin sphere and a water molecule [19]. The intrinsic, nonelectrostatic solute-solute interaction  $U_{\text{ss}}(s)$  can be obtained in a similar fashion. The solvation of the two solutes is studied for a fixed surface-to-surface distance which we define as  $s_0 = r_{12} - 2R_0$ , where  $r_{12}$  is the solute center-to-center distance. We obtain an effective SAS radius of one sphere of about  $R \simeq R_0 + 2.4\text{\AA}$  so that the effective surface-to-surface distance is roughly  $s \simeq s_0 - 4.8\text{\AA}$ . Since we are also interested in the effects of charging up the solutes we place opposite charges  $\pm Ze$ , where  $e$  is the elementary charge, in the center or on the edge of the two spheres.

In the following we focus on a separation distance of  $s_0 = 8\text{\AA}$  to investigate the influence

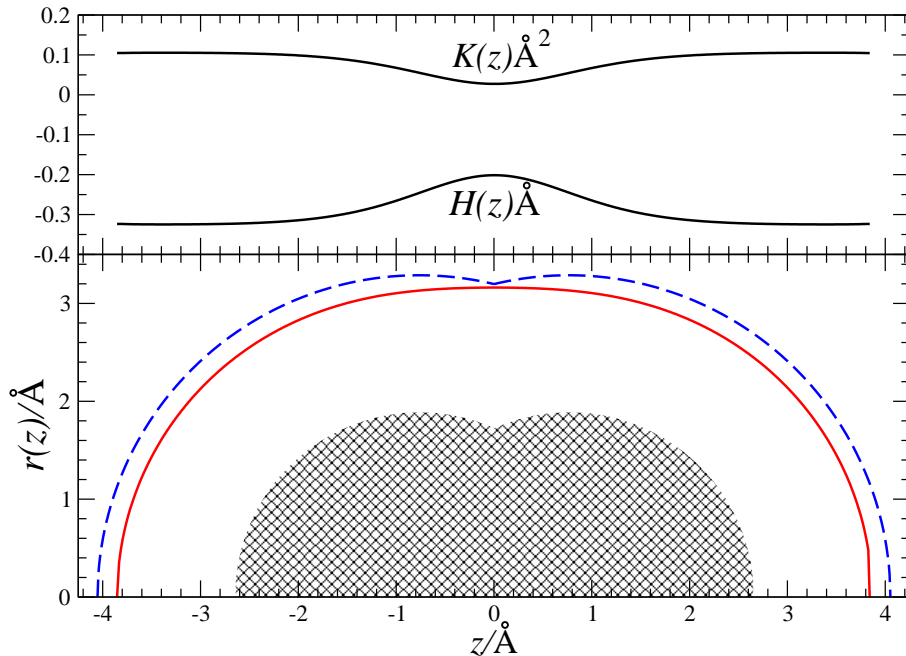


FIG. 1: Mean  $H(z)$  and Gaussian  $K(z)$  curvature and shape function  $r(z)$  (solid lines) for ethane. The canonical SAS (dashed line) from rolling a probe sphere with radius  $r_p = 1.4\text{\AA}$  over the vdW surface (shaded region) is also shown.

of different contributions to the energy functional on the shape function,  $r(z)$ , and the curvatures,  $K(z)$  and  $H(z)$ . For  $s_0 = 8\text{\AA}$ , it follows that  $s \simeq 3.2\text{\AA}$ , such that two water molecules could fit between the solutes on the  $z$ -axis. We systematically change the solute-solute and solute-solvent interactions, as summarized in Tab. I. We begin with only the LJ repulsive interactions in system I and then add a curvature correction with  $\delta = 0.75\text{\AA}$ , vdW attractions, and sphere-centered charges  $Z = 4$  and  $Z = 5$  in systems II-V, respectively. To study the influence of charge location, we shift each charge to the edge of the spheres such that they are  $8\text{\AA}$  apart and reduce their magnitude to  $Z = 1$  (system VI). The surface tension and dielectric constant of the vapor and liquid are fixed to  $\gamma_{lv} = 72\text{mJ/m}^2$ ,  $\epsilon_v = 1$ , and  $\epsilon_l = 78$ , respectively.

The results for the curvatures and SAS, defined by  $r(z)$ , for systems I-VI are shown in Fig. 2. Away from the center of mass ( $|z| \gtrsim 10\text{\AA}$ ) systems I-VI show very little difference.

System	$\delta/\text{\AA}$	vdW attraction	$Z$	$W(s_0)/k_B T$	dewetted
I	0.00	no	0	-57.6	yes
II	0.75	no	0	-34.1	yes
III	0.75	yes	0	-6.3	yes
IV	0.75	yes	4	-9.2	yes
V	0.75	yes	5	-5.1	no
VI	0.75	yes	1 (oc)	-1.3	no

TABLE I: Studied systems for two alkane-assembled spherical solutes.  $W(s_0)$  is the inter-solute pmf. If  $r(z=0) \neq 0$  the system is 'dewetted'. In system VI the solutes' charge is located off-center (oc) at the solute surface.

The curvatures are  $H \simeq -1/R$  and  $K \simeq 1/R^2$  with  $R \simeq 17.4\text{\AA}$ . Close to the center of mass ( $z \simeq 0$ ), however, the influence of changing the parameters is considerable. In system I, Eq. (4) reduces to the minimum surface equation  $H(z) = 0$  for  $z \simeq 0$ . For two adjacent spheres the solution of this equation is the catenoid  $r(z) \simeq \cosh(z)$ , which features zero mean curvature ( $\kappa_1$  and  $\kappa_2$  cancel each other) and negative Gaussian curvature. This leads to a vapor bubble bridging the solutes. When curvature correction is applied (system II) the mean curvature becomes nonzero and positive (concave) at  $z \simeq 0$ , while the Gaussian curvature grows slightly more negative. As a consequence the total enveloping surface area becomes larger and the solvent inaccessible volume shrinks, i.e. the value of the shape function at  $z \simeq 0$  decreases. Turning on solute-solvent dispersion attraction amplifies this trend significantly as demonstrated by system III. Mean and Gaussian curvatures increase fivefold, showing strongly enhanced concavity, and the volume empty of water decreases considerably, expressed by  $r(z=0) \simeq 10.7\text{\AA}$  dropping to  $r(z=0) \simeq 6.3\text{\AA}$ . These trends continue with the addition of electrostatics in system IV. When the sphere charges are further increased from  $Z = 4$  to  $Z = 5$  (system IV  $\rightarrow$  V), we observe a wetting transition: the bubble ruptures and the SAS jumps to the solution for two isolated solutes, where  $r(z \simeq 0) = 0$ . The same holds when going from III to VI, when only one charge,  $Z = 1$ , is placed at each of the solutes' surfaces. Importantly, this demonstrates that the present formalism captures the sensitivity of dewetting phenomena to specific solvent-solute interactions as demonstrated in previous studies [4, 5, 6, 7, 8, 9]. Note that the SAS at  $|z| \simeq \pm 2\text{\AA}$  is closer to the solutes in



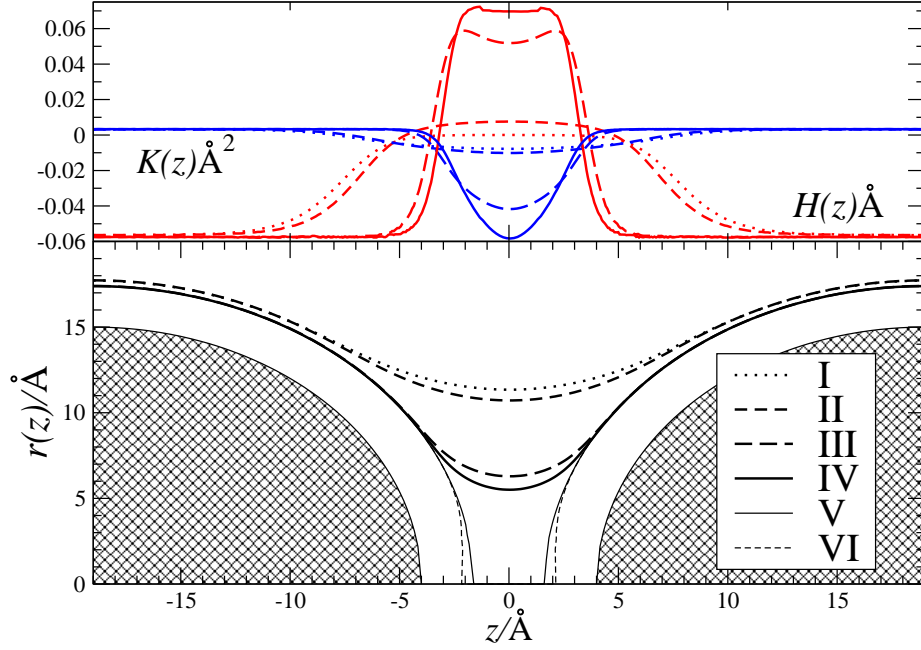


FIG. 2: Mean  $H(z)$  and Gaussian  $K(z)$  curvatures and shape function  $r(z)$  for two alkane-assembled solutes of radius  $R_0 = 15\text{\AA}$  (shaded region) for systems I-VI. Curvatures are not shown for the 'wet' systems V and VI.

VI compared to V due to the proximity of the charge to the interface. Clearly, the observed effects, in particular the transition from III to VI, cannot be described by existing solvation models, which use the SAS [3], or effective surface tensions and macroscopic solvent-solute contact angles [10] as input.

The significant change of the SAS with the solute-solvent interaction has a strong impact on the pmf,  $W(s_0) = G(s_0) - G(\infty) + U_{ss}(s_0)$ . Values of  $W(s_0 = 8\text{\AA})$  are given in Tab. I. From system I to VI the total attraction between the solutes decreases almost two orders of magnitude. Interestingly, the curvature correction (I→II) lowers  $W$  by a large  $23.5k_B T$ , even though  $R \gg \delta$ . A striking effect occurs when vdW contributions are introduced (II→III): the inter solute attraction decreases by  $\simeq 28k_B T$  while the dispersion solute-solute potential,  $U_{ss}(s_0 = 8\text{\AA})$ , changes by only  $-0.44k_B T$ . Similarly, adding charges of  $Z = 5$  (III → V) at the solutes' centers or  $Z = 1$  (III → VI) at the solutes' surfaces decreases the

total attraction by  $1.2k_B T$  and  $6k_B T$ , respectively. Note that the total attraction decreases although electrostatic attraction has been added between the solutes. The same trends have been observed in explicit water simulations of a similar system of charged hydrophobic nanosolutes [7].

These results clearly demonstrate that solvation effects and solvent mediated phenomena are not only strongly influenced by solute-solvent interactions, but that these interactions are inherently coupled. By including coupling, our formalism captures the balance between hydrophobic, dispersive and electrostatic forces which has been observed in previous studies [4, 5, 6, 7, 8, 9] but never described in a single theoretical framework. Nonpolar and polar coupling is expected to be crucial for a complete characterization of biomolecular solvation. The present formalism is only limited by the crude curvature and dielectric descriptions currently employed. Future efforts to improve these approximations will be critical to accurately describe solvation effects on multiple length scales and for more complicated geometries.

The authors thank Tushar Jain, John Mongan, and Cameron Mura for useful discussions. J.D. acknowledges financial support from a DFG Forschungsstipendium. Work in the McCammon group is supported by NSF, NIH, HHMI, CTBP, NBCR, and Accelrys, Inc.

- 
- [1] D. Chandler, Nature (2005), in press, <http://gold.cchem.berkeley.edu:8080/Pubs/DC202.pdf>.
  - [2] G. Hummer et al., Chem. Phys. **258**, 349 (2000).
  - [3] B. Roux, Biophys. Chem. **78**, 1 (1999).
  - [4] X. Huang et al., J. Phys. Chem. B **109**, 3546 (2005).
  - [5] J. Dzubiella and J.-P. Hansen, J. Chem. Phys. **120**, 5001 (2003).
  - [6] S. Vaitheesvaran et al., J. Chem. Phys. **121**, 7955 (2004).
  - [7] J. Dzubiella and J.-P. Hansen, J. Chem. Phys. **119**, 12049 (2004).
  - [8] R. Zhou et al., Science **305**, 1605 (2004).
  - [9] P. Liu et al., Nature **437**, 159 (2005).
  - [10] J. L. Parker et al., J. Phys. Chem. **98**, 8468 (1994).
  - [11] P. Kralchevsky and K. Nagayama, *Particles at Fluid Interfaces and Membranes* (Elsevier, 2001, Amsterdam).
  - [12] T. Chou, Phys. Rev. Lett. **87**, 106101 (2001).

- [13] Y.-K. Cheng and P. J. Rossky, *Nature* **392**, 696 (1998).
- [14] F. H. Stillinger, *J. Solution Chem.* **2**, 141 (1973).
- [15] A. Nicholls et al., *Proteins* **11**, 281 (1991).
- [16] D. M. Huang et al., *J. Phys. Chem. B* **105**, 6704 (2001).
- [17] E. Gallicchio et al., *J. Phys. Chem. B* **104**, 6271 (2000).
- [18] H. S. Ashbaugh et al., *Biophys. J.* **75**, 755 (1998).
- [19] D. M. Huang and D. Chandler, *J. Phys. Chem. B* **106**, 2047 (2002).